universität wien

MASTERARBEIT | MASTER'S THESIS

Titel | Title

Ecological Relevance of Extracellular Vesicles in the Northern Adriatic Sea

verfasst von | submitted by

Mirjam Aubert BSc

angestrebter akademischer Grad | in partial fulfilment of the requirements for the degree of

Master of Science (MSc)

Wien | Vienna, 2025

Studienkennzahl lt. Studienblatt | Degree programme code as it appears on the student record sheet:	UA 066 833
Studienrichtung lt. Studienblatt | Degree programme as it appears on the student record sheet:	Masterstudium Ecology and Ecosystems
Betreut von | Supervisor:	Univ.-Prof. i.R. Dr. Gerhard Herndl

Table of contents

Acknowledgements

I would like to thank Gerhard J. Herndl for making this thesis possible. Thank you for making this short research trip feasible, for your continued support and your constructive feedback. I would also like to thank Eduard Fadeev for arranging this short research trip. Thank you for giving me an insight into the complete planning, execution and evaluation of a collaborative project and for the great support throughout. I would also like to thank Tinkara Tinta, Neža Orel, Mauro Celussi and Cécile Carpaneto Bastos for the realization of this project and the support during the sampling and the analysis. Many thanks also to the Microbial Oceanography group for their support and willingness to help. And finally, a very special thanks to my mother for her unconditional support through all of the ups and downs during my studies.

Abstract

Over the last years it has been recognized that extracellular vesicles (EV) might be abundant on the marine environment. Their ecological role in the ocean, however, remains largely enigmatic. We investigated the abundance and potential contribution of EV-like particles to the microbial food web in the North Adriatic Sea. Specifically, we determined the nutrient content and extracellular enzymatic activity associated with nanoparticles to the amount of EV-like particles contained in the size range of nanoparticles. It was found that up to 30% of total nanoparticles can be characterized as EV-like particles and for each bacterial cell we counted up to 4 EVs. From all investigated dissolved nutrients 6% could be directly attributed to nanoparticles. Furthermore, the extracellular enzymatic activity assay indicated that at least part of the extracellular enzymes is associated with nanoparticles. Considering the spatial and temporal consistency of EV concentrations, our findings indicate that EVs might serve both as nutrient and enzymatic activity hotspots in marine surface waters.

Key words: extracellular vesicles, nanoparticles, extracellular enzymatic activity, marine bacteria, nutrient hotspots

Zusammenfassung

In den letzten Jahren hat man erkannt, dass extrazelluläre Vesikel (EV) in marinen Ökosystemen reichlich vorhanden sein können. Ihre ökologische Rolle im Meer bleibt jedoch weitgehend rätselhaft. Wir untersuchten die Häufigkeit und den möglichen Beitrag von EV-ähnlichen Partikeln zum mikrobiellen Nahrungsnetz in der Nordadria. Dazu bestimmten wir den Nährstoffgehalt und die extrazelluläre enzymatische Aktivität, die mit den Nanopartikeln assoziiert sind und verglichen die Werte mit dem Anteil an EV-ähnlichen Nanoartikeln zu der Gesamtzahl von Nanopartikeln. Es zeigte sich, dass bis zu 30 % der gesamten Nanopartikel als EV-ähnliche Partikel charakterisiert werden können, und für jede Bakterienzelle zählten wir bis zu 4 EVs. Von allen untersuchten gelösten Nährstoffen konnten 6 % direkt auf Nanopartikel zurückgeführt werden. Darüber hinaus zeigte sich, dass zumindest ein Teil der extrazellulären Enzyme mit Nanopartikeln assoziiert ist. In Anbetracht der räumlichen und zeitlichen Konsistenz der EV-Konzentrationen deuten unsere Ergebnisse darauf hin, dass EVs sowohl als Nährstoff- als auch als Enzymaktivitäts-Hotspots in marinen Oberflächengewässern dienen könnten.

Schlagwörter: extrazelluläre Vesikel, Nanopartikel, extrazelluläre enzymatische Aktivität, marine Bakterien, Nährstoff-Hotspots

Introduction

Extracellular vesicle (EV) production and release can be found in all three branches of the tree of life and occur in a variety of environments (Deatherage & Cookson 2012). The size of the spherical, membrane-bound structures released by bacteria, archaea, and eukaryotes ranges from 10 - 300 nm (Biller, 2020, Deatherage & Cookson 2012; Kulp & Kuehn 2010). In terms of size, they are therefore part of the "dissolved" fraction of organic matter in aquatic ecosystems (Verdugo et al. 2004). It has been demonstrated that both gram-negative as well as gram-positive bacteria release membrane vesicles (MVs), as bacterial EVs are referred to. In gram-negative bacteria, MVs are produced by outer membrane blebbing or by cell lysis and are referred to as outer membrane vesicles (OMVs) or outer-inner membrane vesicles (Nagakubo et al. 2019, Toyofuku 2019). As vesicles extracted from natural environments can have various origins and biogenesis, they will be referred to as EVs in the course of this analysis (MISEV 2018 guidelines; Thiéry et al. 2018).

The outer membrane of most gram-negative bacteria is composed of lipopolysaccharides in the outer leaflet and phospholipids in the inner leaflet (Bos et al. 2007). During active growth of bacteria, small portions of the outer membrane bulge away from the cell and detach, encapsulating periplasmic luminal components (Kulp & Kuehn 2010). The resulting bacterial EVs are 20-250 nm in size (Schwechheimer 2015; Kulp & Kuehn 2010). The content of EVs underlines that their biogenesis is an active process and not a by-product of cell lysis as protein analyses revealed a high depletion of inner membrane and cytoplasmic components (McBroom & Kuehn 2005, Kulp & Kuehn 2010; Schwechheimer 2015). EVs can contain a multitude of cargo such as DNA, RNA, plasmids and toxins and can play multi-functional roles in various cell-cell interactions (Biller et al. 2022; Ellis & Kuehn 2010; Hagemann et al. 2013; Kulp & Kuehn 2010; Li et al. 2016; Lynch & Alegado 2017; Manning & Kuehn 2011; Schatz & Vardi 2018). Containing nucleic acids, it is important to consider EVs in ecological studies of viruses, as size fractionation cannot separate phages from EVs. It has been shown that EVs can mimic viral particles in epifluorescence microscopy (EFM) analyses and therefore leading to overestimations of viral abundances in samples from the natural environment (Hagemann et al. 2013; Soler et al. 2008, 2015).

In marine environments, EVs are abundant in coastal and oligotrophic open waters and numerous marine bacteria isolated from mid-latitudes and polar regions as well as marine sediments are releasing EVs in laboratory cultures (Baeza & Mercade 2020; Biller 2020; Biller et al. 2014, 2017, 2021, 2022; Fadeev et al. 2023; Frias et al. 2016; Hagemann et al. 2013; Kwon et al. 2016; Li et al. 2016; Naval & Chandra 2019, Nekrouf et al. 2025). Marine EVs can be associated with biofilms as well as with free-living bacteria (Biller 2020; Schooling & Beveridge 2006). Biller et al. (2014; 2023) described depth dependent vesicle dynamics in the ocean where vesicle-like particles in the surface waters can be found in abundances comparable to bacterial cells and in decreasing numbers with water

column depth and the corresponding decrease in solar radiation and temperature. Their potential to contribute to marine food webs as hotspots of dissolved organic nutrients and labile dissolved organic carbon is highlighted through experiments by Biller et al. (2014), where they revealed that the two marine heterotrophic bacteria *Alteromonas* and *Halomonas* could grow on *Prochlorococcus* vesicles as the only carbon source, which illustrated that at least some of the vesicles' carbon is labile (Biller et al. 2014; Lynch & Alegado 2017). Supporting the ecological relevance of MVs are the findings of Fadeev et. al (2023) which revealed that MVs of *A. macleodii* harbor a considerable amount and diversity of enzymes that are linked to bacterial extracellular enzymatic activity (EEA) which comprised up to 20% of the total EEA in the culture.

Based on previous studies where EVs could be isolated from various marine environments and several marine microbial EV producers were identified, we hypothesized to be able to identify EV-like nanoparticles in the surface waters of the Northern Adriatic Sea. The biogenesis of EVs indicates that at least part of the dissolved nutrients measured in seawater might be associated to nanoparticles such as EVs. This was investigated by measuring dissolved organic carbon (DOC), total dissolved nitrogen (TDN), and total soluble phosphorus (TSP). Being bulged off from gram-negative cell membranes as a common way of vesicle formation, encapsulating periplasmic proteins and harboring ectoenzymes, we further determined extracellular enzymatic activity (EEA) associated with high molecular weight nanoparticles such as EV-like particles (Fadeev et al. 2022).

Material and Methods

Sampling site and sampling intervals

Sampling was conducted in the Gulf of Trieste, the northernmost part of the Adriatic Sea. The shallow, river-dominated ecosystem with an average depth of 23 m is well mixed in winter but stratified in summer. The highest freshwater input comes from the Soča (Isonzo) River (Malačič et al. 2006). Over the timespan of three days in August 2022 (01/08/2023, 03/08/2023, 05/08/2023), three stations representing a gradient along a transect off Piran, Slovenia, were sampled (Fig. 1). At each station, temperature, salinity and dissolved oxygen were measured with a CTD fine-scale probe (Microstructure profiler MSS90, Sea & Sun Technology GmbH). The seawater was collected at the thermocline at about 10 m depth. For each station 30 L of seawater were collected with a rosette of 5 L Niskin bottles and stored in 1 M HCl and Milli-Q pre-washed Nalgene bottles, protected from solar radiation.

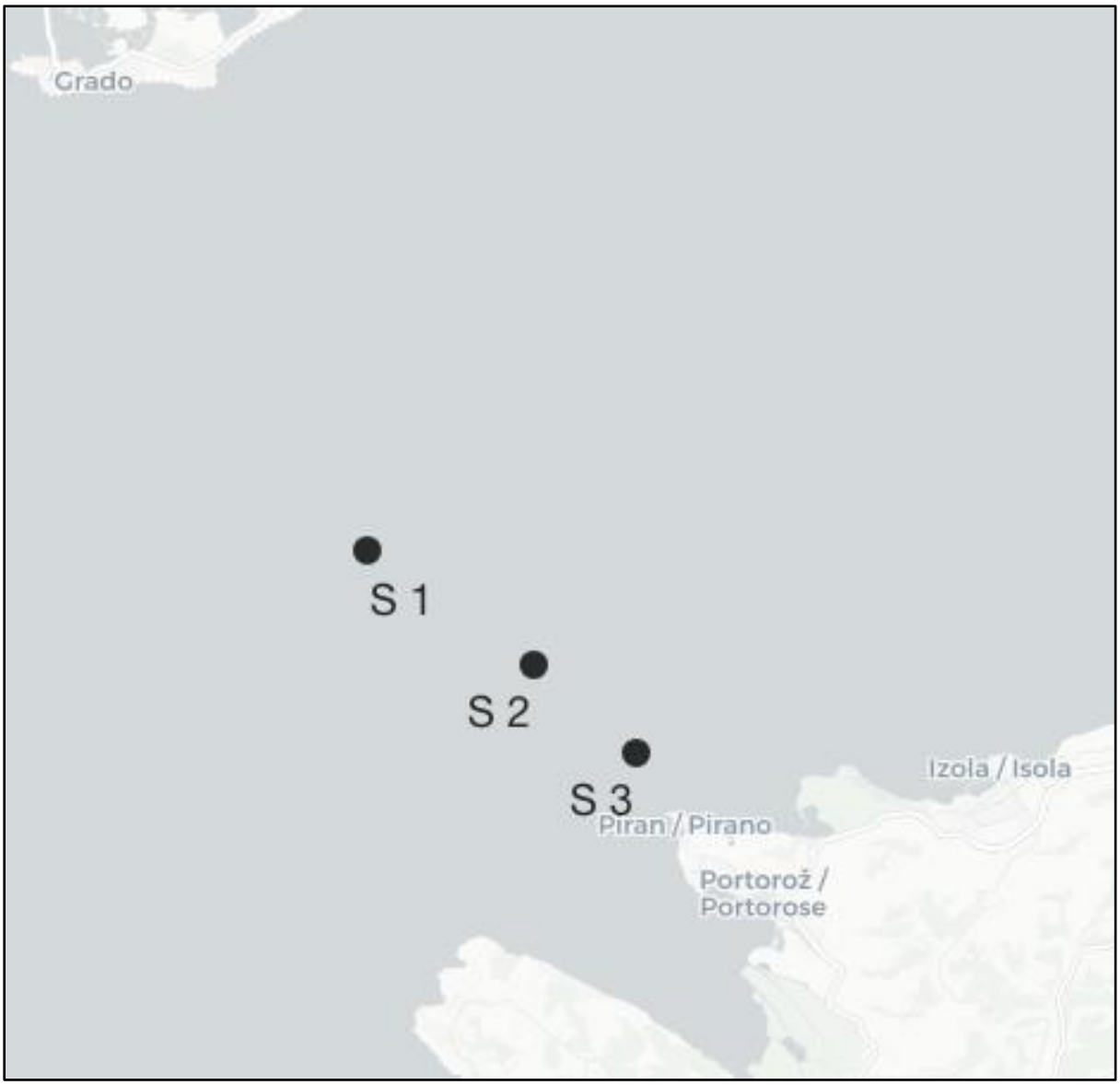

Figure 1. Transect of the sampling locations in the Gulf of Trieste: station 1 (S1; 45° 35.000'N 13° 28.600E'), station 2 (S2; 45° 33.600'N, 13° 31.500'E), and station 3 (S3; 45° 32.555'N 13°33.252'E).

After returning to the lab, all seawater samples were pre-filtered through 142 mm 5 µm pore-size polycarbonate membranes with a low-pressure filtration system. On the third sampling day, pre-filtration was conducted with 142 mm 3 µm pore-size polycarbonate membranes.

Microbial abundance

For microbial abundance measurements, 1.5 mL of the pre-filtered seawater were collected into a 2 mL cryovial, fixed with glutaraldehyde (final concentration 2.5 %, 10 min incubation), flash-frozen with liquid nitrogen and stored at -80°C until further analysis. After thawing at room temperature, the

samples were stained with SYBR Green I (Invitrogen, Burlington, ON, Canada) and the microbial abundance was determined on a FACSAria Cell Sorter (BD Biosciences, Canada) (Brussaard 2004, Marie et al. 1999).

Heterotrophic bacterial carbon production (BCP)

Four mL of the pre-filtered seawater were used to determine the heterotrophic bacterial carbon production (BCP). Using the ^{3}H leucine incorporation method (20 nM final concentration, Perkin-Elmer) BCP was measured following the centrifugation protocol of Smith and Azam (1989). As described by Simon and Azam (1992) the dilution factor of 2 and the conversion factor of 1.55 kg C per mol leucine was used to calculate BCP (Lee and Fuhrman, 1987).

Quantification and size estimation of nanoparticles

To enumerate the total number of nanoparticles in the sample, the pre-filtered seawater was filtered through a 0.22 µm polycarbonate membrane and a 15 mL subsample for nanoparticle tracking analysis (NTA) stored at 4°C in the dark. On the last sampling day, the polycarbonate membranes were exchanged for 0.22 µm mixed cellulose ester membranes due to operational matters. For the differentiation of high molecular weight (HMW) particles from the truly dissolved fraction (< 100 kDa), the remaining pre-filtered seawater was concentrated 100x on a 100 kDa membrane with a VivaFlow system (Merck, Germany). Subsamples of 15 mL were taken from the concentrated fraction as well as from the < 100 kDa outflow for NTA and stored at 4°C in the dark. Another 15 mL subsample was taken for density gradient fractionation and stored at 4°C in the dark. The remaining concentrated seawater was loaded onto 100 kDa MWCO Vivaspin tubes (Merck, Germany) and concentrated as much as the samples allowed for later molecular analysis (not included in the thesis).

Separation of EV-like and virus-like nanoparticles by density gradient fractionation

To differentiate the nanoparticles of the HMW subsample (100 kDa - 0.22 µm) between EV-like and virus-like particles, particles were isolated and purified based on the isolation protocol of Biller et al. (2022). The 15 mL subsamples for density gradient fractionation were concentrated to 3 mL with 100 kDa Vivaspin tubes to load them on an iodixanol density gradient. The OptiPrep density gradient (Merck, Germany) was prepared in ultracentrifuge tubes by overlying equal volumes (1 mL) of iodixanol dilutions (0 %, 10 %, 15 %, 20 %, 25 %, 30 %, 35 %, 40 %, 45 %) made by dilution of 60% iodixanol with 4x phosphate-buffered saline (PBS). The 3 mL of the concentrated sample were carefully added on top of the gradient and centrifuged in an ultracentrifuge at 100,000x *g* in 4°C for 6 h. Extensive preliminary experiments with EVs produced by *Alteromonas macleodii ATCC,* different phages and natural seawater samples, in addition to first results of the protein analysis of the samples taken in the

Gulf of Trieste identified the EV-like particles accumulating at densities between 15-40 % iodixanol (1.055 - 1.199 g mL^{-1}). The virus-like particles were identified in the 45 % iodixanol concentration and accumulated in the pellet (1.251 - 1.397 g mL^{-1}). For NTA, the nanoparticles had to be extracted from the density gradient and the iodixanol needed to be replaced by 1x PBS. To do so, the fractions containing EV-like particles (15-40 % iodixanol) as well as the ones containing virus-like particles (45% iodixanol plus pellet) were pipetted separately into 100 kDa Vivaspin tubes (Merck, Germany), topped up to 20 mL with pre-filtered 1x PBS, and centrifuged at 805x *g* for 20 min. After discarding the < 100 kDa outflow, this washing step with 1x PBS was repeated. The concentrates were collected in 2 mL Eppendorf vials, topped up to a final volume of 1 mL with 1x PBS and stored at 4°C until NTA was conducted.

Nanoparticle tracking analysis

The abundance and size distribution of the nanoparticles were measured by NTA using a NanoSight NS300 instrument (Malvern Panalytical Ltd.) equipped with a blue laser module (wavelength: 488 nm) and the NTA 3.4 software. The samples were loaded with a syringe load speed of 50 and five 60 sec videos were recorded for each sample. The videos for the samples containing nanoparticles from 100 kDa - 0.22 µm were recorded and processed in light scatter mode with a screen gain of 1, camera level of 16 and detection threshold of 5. For the particles extracted from the iodixanol density gradient, the neutral density mode was selected instead of light scatter mode to optimize particle detection. All other settings remained the same. For the interpretation of the results, all concentrations necessary for the NTA measurements were calculated back to the natural concentrations in the seawater samples.

Chemical parameters

To determine the chemical parameters associated with the total nanoparticles in the samples, 100 mL of the pre-filtered seawater was filtered through combusted 25 mm GF/F membranes using a glass filtration set (1M HCl, Milli-Q pre-washed and combusted). From the GF/F filtrate, 2 x 30 mL were collected into combusted 40 mL glass vials for dissolved organic carbon (DOC) and total dissolved nitrogen (TDN) analysis and stored at -20°C until analysis. From the 100 kDa - 0.22 µm fraction, another 30 mL were prepared in the same way and from the < 100 kDa another 2 x 30 mL were prepared and stored at -20°C. For the analysis, the samples were thawed and acidified with 12 M HCl to a final pH below 2. The analysis was performed with a high-temperature catalytic method using a Shimadzu TOC-L analyzer equipped with a total nitrogen unit (Hansell and Carlson 1998) . For the analysis of the total soluble phosphorus (TSP), 15 mL of the GF/F filtered sample prepared for DOC/TDN analysis

were collected into a rinsed 15 mL Greiner tube and stored at -20°C. The samples were measured using the ascorbic acid-molybdenum blue method for soluble reactive phosphorus analysis (Awwa 1998).

Extracellular enzymatic activity (EEA)

To measure the EEA as promptly as possible after returning to the lab, a subsample of 160 mL of the pre-filtered seawater was filtered through 25 mm 0.22 µm membranes by syringe filtration. To verify that the filtrate was cell-free, 500 µL were fixed with 20 µL 25% glutaraldehyde, stained with x100 SYBR Green (Sigma-Aldrich), and measured on a BD AccuriTM C6 flow cytometer (BD Biosciences). From this cell-free filtrate 15 mL were collected in a clean 15 mL tube and used for EEA analysis. To verify the concentration of nanoparticles, another 15 mL were collected for NTA and stored in the dark at -20°C. From the remaining filtrate, 120 mL were loaded onto 100 kDa MWCO Vivaspin tubes (Merck, Germany) and concentrated for 20 min at 695 x g. The concentrate was topped up to 20 mL with pre-filtered (0.22 µm) artificial seawater (ASW). Fifteen mL were collected in a clean 15 mL tube and used for the EEA measurement. The remaining 5 mL were stored in the dark at -20°C in another 15 mL tube for NTA. From the < 100 kDa outflow, 15 mL were collected in a clean tube for EEA measurements and 15 mL for NTA stored in the dark at -20°C until further analysis.

Extracellular enzymatic activities were assayed using fluorogenic substrate analogues (Hoppe, 1993) at each sampling day on the size fractions: < 3 µm, < 0.2 µm, 100 kDa - 0.22 µm, and < 100 kDa. Leucine aminopeptidase (LEU) activity was assayed as the hydrolysis rate of leucine-AMC. β-glucosidase (BETAGLU), olease (OLE), chitinase (CHIT), and alkaline phosphatase (AP) activities were assayed using the substrates MUF-β-D-glucoside, MUF-oleate, MUF-N-acetyl-β-D-glucosaminide and MUF-phosphate, respectively (Sigma Aldrich®). Hydrolysis was measured by incubating 0.3 mL aliquots with 200 µM MUF-β-D-glucoside, MUF-α-D-glucoside, MUF-N-acetyl-β-D-glucosaminide, leucine-MCA, 100 µM MUF-oleate and 50 µM MUF-phosphate (saturating final concentrations) in the dark at the experimental temperature for 1-2 h. These concentrations have been proven to be saturating in previous studies in the Adriatic Sea (Celussi and Del Negro, 2012; Celussi et al., 2015). All samples were run in five replicates. Triplicate calibration curves were performed using 0.2 µm filtered seawater and 5 µM MUF and MCA standard solutions.

Results

Bacterial abundance and heterotrophic production

Bacterial abundance at the three stations ranged from $2.3x10^8$ to $6.0x10^8$ cells L^{-1} and no recurrent spatial or temporal pattern was detected. On the first sampling day, the number of cells measured showed a decline in abundance from the station furthest away from the coast (S1) with $4.8x10^8$ cells L^{-1} to the one closest (S3) to the coast where the overall lowest cell abundance of $2.3x10^8$ L^{-1} was measured. On the third sampling event, where the samples were pre-filtered through 3 µm, compared to 5 µm for the first two events, the mean cell abundance of the three stations was $5.3x10^8 \pm 6.7x10^7$ cells L^{-1}, twice as high as on the second day ($2.4x10^8 \pm 6.0x10^6$ cells L^{-1}) (Fig. 2A). The measured bacterial carbon production (BCP) ranged between 1.2 ± 0.94 µg C L^{-1} d^{-1} and 7.5 ± 0.04 µg C L^{-1} d^{-1}. The average carbon production of day 2 (5.5 ± 0.10 µg C L^{-1} d^{-1}) was three times as high compared to day 1 (1.8 ± 0.37 µg C L^{-1} d^{-1}) and day 3 (1.8 ± 0.10 µg C L^{-1} d^{-1}). On the first and the third sampling event, station 2 showed a slight decrease in BCP compared to the other two stations. However, this spatial pattern is not reflected in the second sampling event (Fig. 2B). Comparing the bacterial abundance with the BCP, there were no distinct spatial or temporal patterns detectable (Fig. 2A & B).

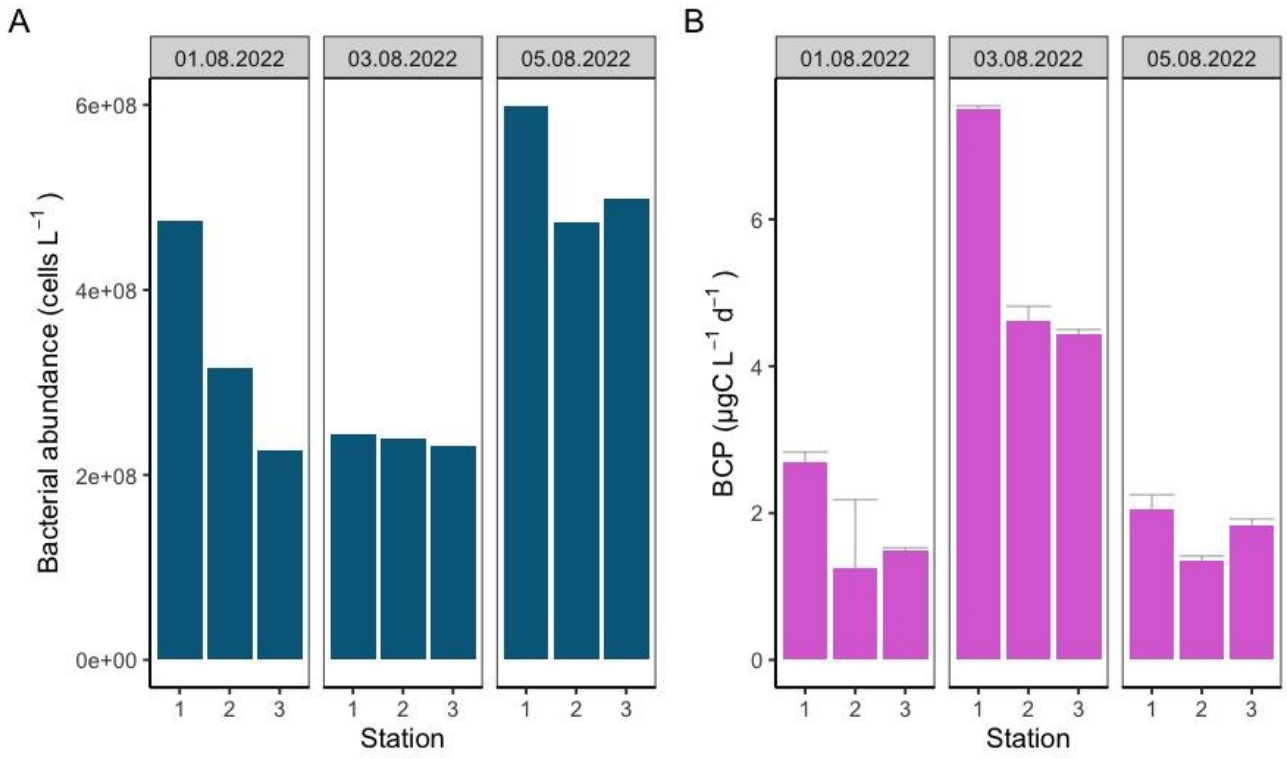

Figure 2. Bacterial abundance and bacterial carbon production (BCP) measured at stations 1-3 on three sampling events. The cell abundance (A) was measured by flow cytometry and the BCP (B) was determined by leucine incorporation.

Nanoparticle and extracellular vesicle abundance

Nanoparticles were quantified by nanoparticle tracking analysis (NTA). The total nanoparticles retained in the size fraction of 100 kDa - 0.22 µm were enumerated. From the same size fraction EV-like nanoparticles and virus-like nanoparticles were obtained by density gradient fractionation and enumerated as well.

The concentrations of total nanoparticles measured in the size fraction of 100 kDa - 0.22 µm ranged from $2.4x10^6 \pm 4.6x10^4$ to $1.1x10^7 \pm 1.7x10^5$ particles mL^{-1}. A recurring spatial pattern can be seen on the second and third sampling event, where the concentration of total nanoparticles decreased with increasing proximity to the coast. This pattern in concentrations, however, was reversed on the first sampling event. EV-like nanoparticles were detected in every sample ranging from $5.9x10^4 \pm 4.7x10^3$ up to $9.7x10^5 \pm 7.0x10^4$ particles mL^{-1} (Fig. 3). Besides station 3 on the second sampling event, the concentration of EV-like particles was fairly stable and did not mirror the numbers of total nanoparticles measured in the same sample. The concentrations of the denser virus-like particles were in a similar range as the concentration of EV-like particles on the first sampling event and also at station 1 and 2 sampled on the second sampling day with concentrations of $3.3x10^5 \pm 1.9x10^4$ to $1.1x10^6 \pm 4.2x10^4$ particles mL^{-1}. For station 3 on sampling event 2 and at all stations on the third sampling event the concentration on virus-like particles was relatively low compared to EV-like particles (Fig. 3).

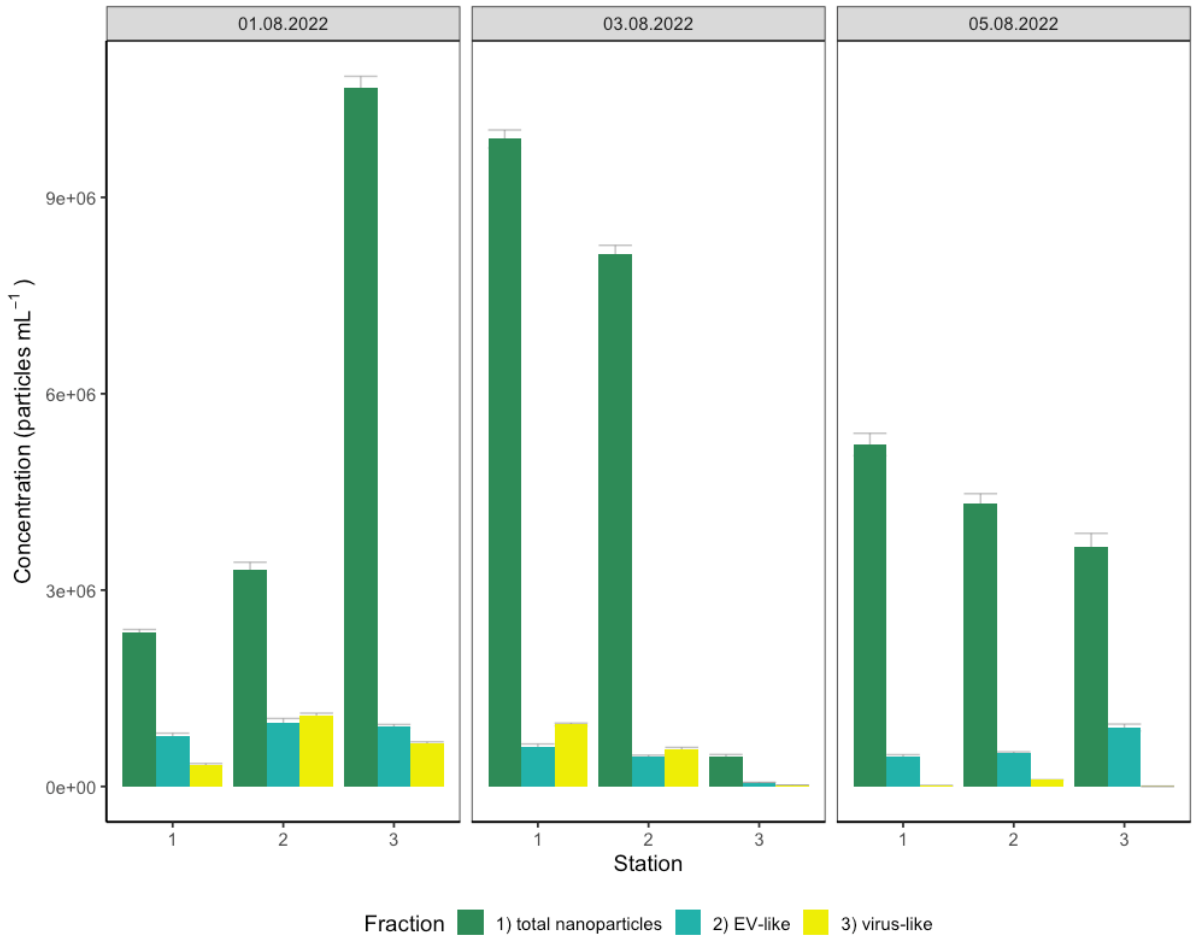

Figure 3. Concentration of total nanoparticles, EV-like nanoparticles, and virus-like nanoparticles. Concentration of nanoparticles (green) from the 100kDa - 0.22 µm size fraction, EV-like (blue) and virus-like (yellow) nanoparticles measured at three sampling events on the three sampling stations.

EV-like nanoparticles were found to be predominantly in the size range between 100 to 150 nm with a peak at 120 nm. Virus-like particles peaked at 110 nm and 170 nm (Fig. 4).

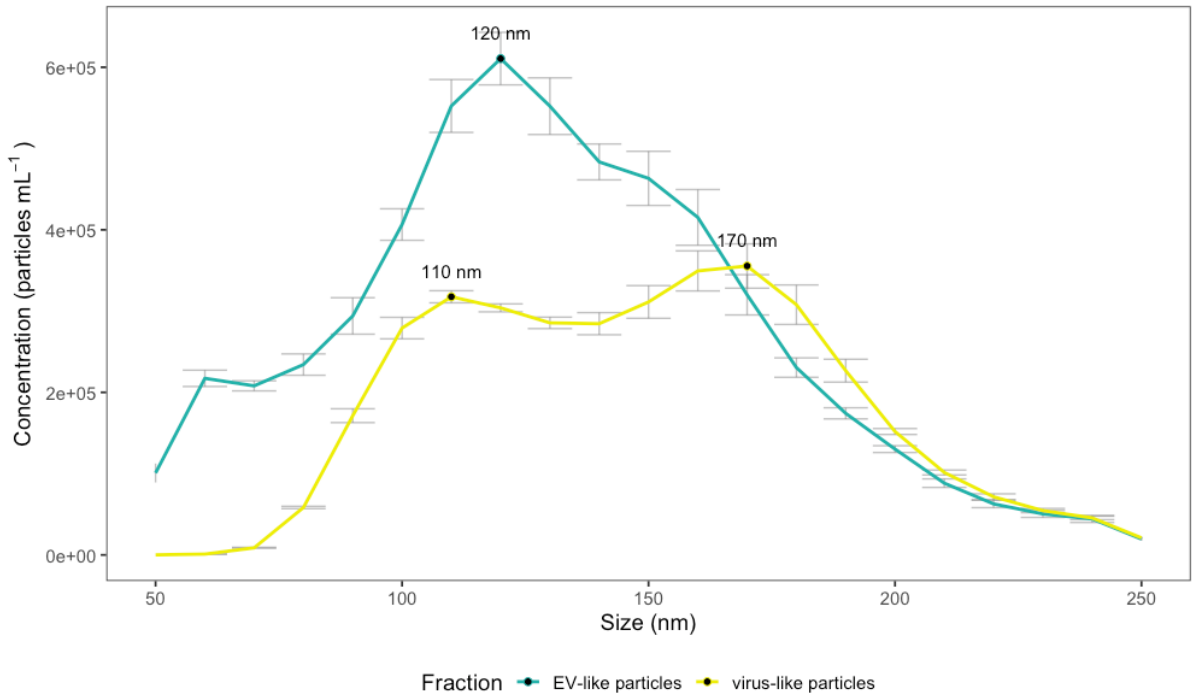

Figure 4. Size distribution of EV-like nanoparticles and virus-like nanoparticles. Average size distribution of EV-like nanoparticles (blue) and virus-like nanoparticles (yellow) over all samples.

Dissolved nutrients

Figure 5 shows the DOC, TDN, and total soluble phosphorus (TSP) concentration associated with nanoparticles. The concentrations measured in the < 100 kDa fraction were subtracted from the measured concentrations in the fraction 100 kDa - 0.22 µm to obtain the concentration in nanoparticles. On the second sampling day all measured organic matter concentrations at station 3 were close to zero or below detection threshold. The measured DOC concentrations for the other days and stations ranged from 5.7 µmol L^{-1} to 9.1 µmol L^{-1}. The average DOC concentration associated with total nanoparticles was 7.2 ± 3.0 µmol L^{-1} (Fig. 5A). The concentrations of TDN ranged from 0.01 µmol L^{-1} measured at station 2 on the second sampling day up to 0.6 µmol L^{-1} measured at station 3 on the first sampling day (Fig. 5B). The same pattern could be seen for the TSP. The measurement from the samples from station 3 on the second sampling day was below detection threshold and the highest concentration was measured on the first day at station 3 with a concentration of 0.007 µmol L^{-1} (Fig. 5C). Overall, the measured variations in concentrations of organic matter are consistent with the number of nanoparticles detected in the size fractions of 100 kDa - 0.22 µm. The decrease in virus-like particles and the low concentration of organic matter on the second sampling event at station 3 will both be addressed in the discussion (Fig. 3 & 5).

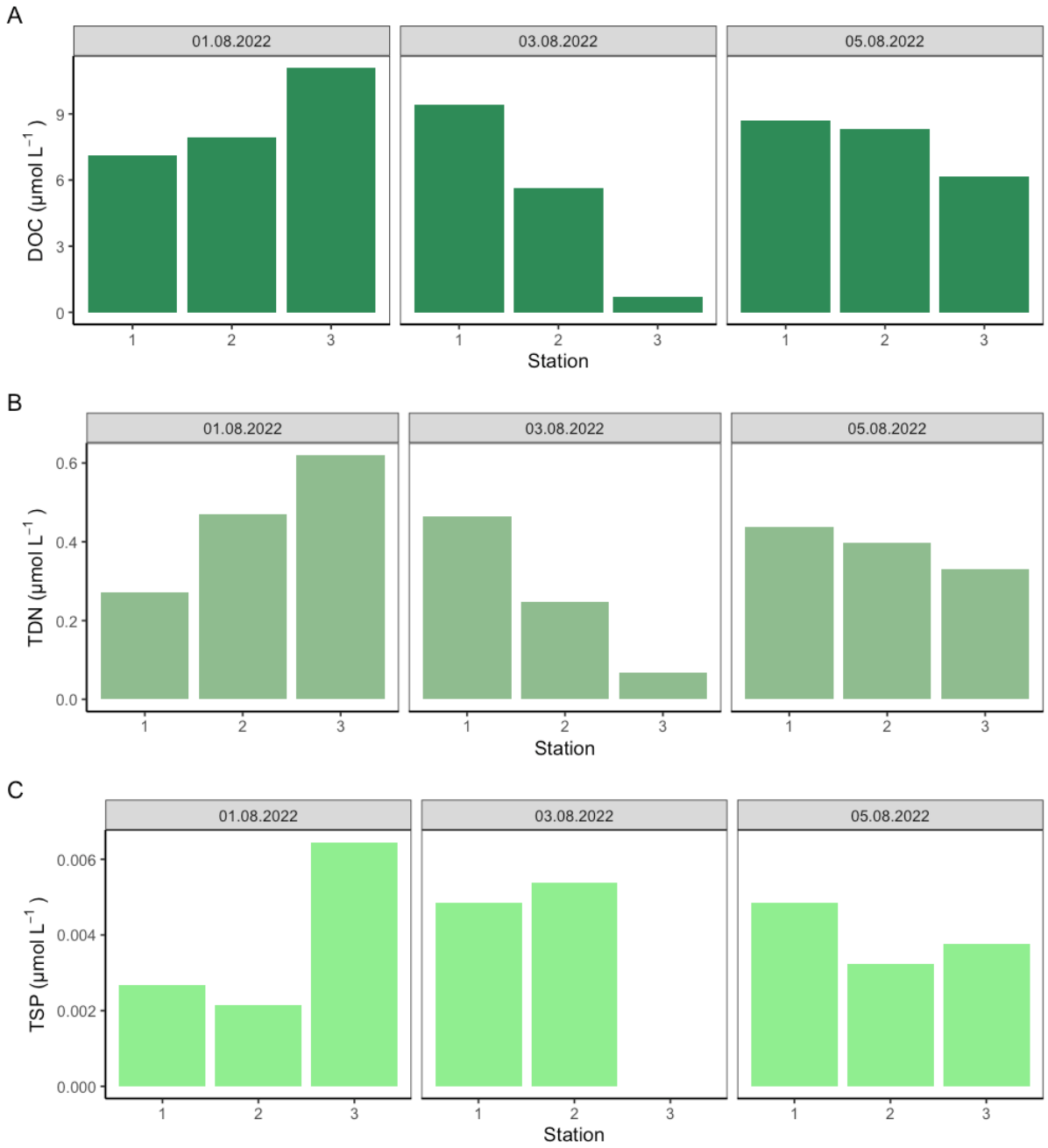

Figure 5. Spatio-temporal dynamics of DOC, TDN, and TSP associated with nanoparticles. DOC (A), TDN (B), and TSP (C) were measured on the size fractions 100 kDa - 0.22 µm and < 100 kDa. The < 100 kDa background was then subtracted from the 100 kDa - 0.22 µm measurements to obtain the concentrations associated with nanoparticles only. All parameters were measured on stations 1-3 on three sampling events.

The average DOC, TDN, and TSP concentrations measured in the cell-free (< 0.22 µm) size fraction were 117.6 ± 10.4 µmol L^{-1}, 5.6 ± 1.4 µmol L^{-1}, and 0.06 ± 0.06 µmol L^{-1}, respectively. Overall, 6.2 ± 2.7% of the total DOC, 6.6 ± 2.8% of the TDN and 6.7 ± 6.4% of the TSP was contained in

nanoparticles (Table 1). The ratio of DOC to TDN in the cell free (< 0.22 µm) fraction was 22:1, while this ratio for nanoparticles was 20:1.

Table I. Average nutrient concentrations in the different fractions. Average concentrations of nutrients (DOC, TDN, TSP) measured in the cell-free (< 0.22 µm) size fraction and nutrients contained in nanoparticles were obtained by subtracting the truly dissolved nutrients (< 100 kDa) from the concentrations in the 100 kDa – 0.22 µm size fraction. Percentage of nutrients of the cell-free fraction contained in nanoparticles.

	Cell-free (< 0.22 µm)	**Purely from nanoparticles**	**Percentage (%)**
Mean DOC (µmol L^{-1})	117.6 ± 10.4	7.2 ± 3.0	6.2 ± 2.7
Mean TDN (µmol L^{-1})	5.6 ± 1.4	0.4 ± 0.2	6.6 ± 2.8
Mean TSP (µmol L^{-1})	0.06 ± 0.06	0.004 ± 0.002	6.7 ± 6.4

Figure 6 shows the dissolved organic matter concentrations in nanoparticles. The DOC concentrations ranged between 0.7 to 3.0 µmol carbon per 10^6 nanoparticles with an average DOC concentration of 1.7 ± 0.7 µmol per 10^6 nanoparticles (Fig. 6A). The average TDN concentration was 0.09 ± 0.04 µmol per 10^6 nanoparticles ranging from 0.03 to 0.14 µmol per 10^6 nanoparticles (Fig. 6B). Besides the measurement from station 3 on the second sampling day being below detection threshold, TSP per 10^6 nanoparticles did not display remarkable spatial or temporal variations averaging 0.0008 ± 0.0002 µmol TSP per 10^6 nanoparticles (Fig. 6C).

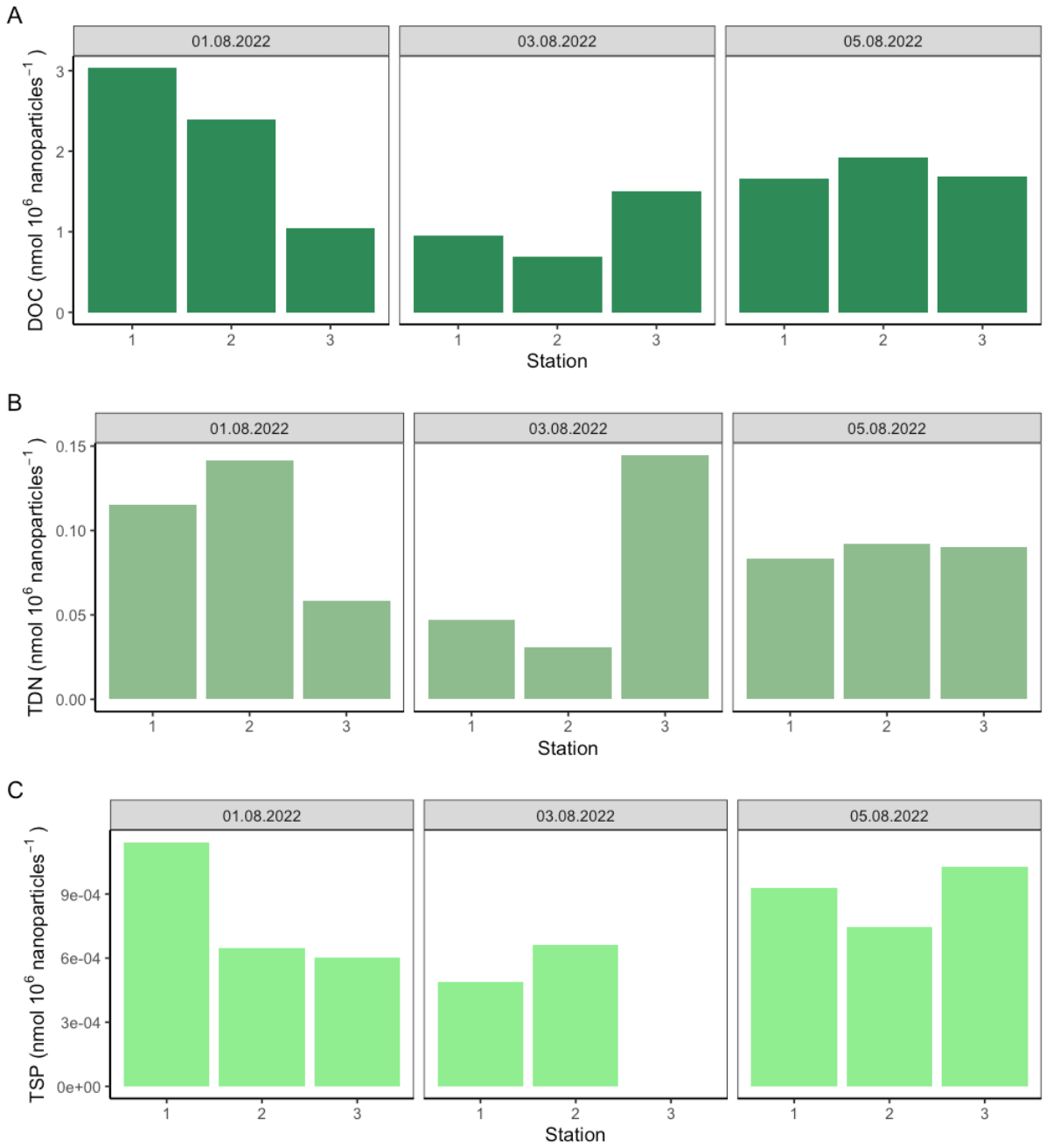

Figure 6. DOC, TDN, and TSP per 106 nanoparticles. DOC (A), TDN (B) and TSP (C) concentrations of Fig. 5 were used to calculate the amount of dissolved nutrients contained in 10^6 nanoparticles.

Extracellular enzymatic activity (EEA)

Extracellular enzymatic activity assays for LEU, BETAGLU, OLE, CHIT, and AP activities were conducted for all three stations on each sampling event. The nanoparticle enumeration by NTA showed that the concentration of nanoparticles by tangential flow filtration in Amicon tubes with 100 kDa membranes only worked on the third day of sampling. Therefore, we focused the analysis of the

EEA on the third sampling event. The EEA measured in the cell-free fraction < 0.22 µm was compared to the EEA associated with nanoparticles of the size fraction 100 kDa - 0.22 µm and the outflow of the 100 kDa tangential flow filtration. To minimize the background EEA for the EEA measurements associated with nanoparticles, the samples that were first concentrated on a 100 kDa membrane and then diluted 20x with artificial seawater.

The highest EEA in the < 0.22 µm cell-free fraction and associated with nanoparticles was measured for OLE with 55.0 ± 3.5 nmol L^{-1} h^{-1} and 9.9 ± 1.3 nmol L^{-1} h^{-1},respectively (Fig. 7). The mean EEA of AP in the cell-free fraction (0.22 µm) was 2-fold higher at station 1 compared to station 2 and 3.The measured EEA of AP associated with nanoparticles was similar between all stations with a mean of 0.29 ± 0.10 nmol L^{-1} h^{-1}. For LEU a mean EEA of 3.1 ± 0.9 nmol L^{-1} h^{-1} was measured in the cell-free fraction. The mean EEA associated with nanoparticles was ten-fold lower (0.35 ± 0.03 nmol L^{-1} h^{-1}). With a mean of 2.7 ± 0.6 nmol L^{-1} h^{-1} the EEA of CHIT in the cell-free fractions was also ten-fold higher than the EEAs associated with nanoparticles (mean of 0.26 ± 0.3 nmol L^{-1} h^{-1}). BETAGLU EEA was very low (0.3 ± 0.1 nmol L^{-1} h^{-1}) in the cell-free fraction (< 0.22 µm). For all substrates the EEA measured in the < 100 kDa fraction was very similar to the EEA measured in the cell-free fraction (Fig. 7).

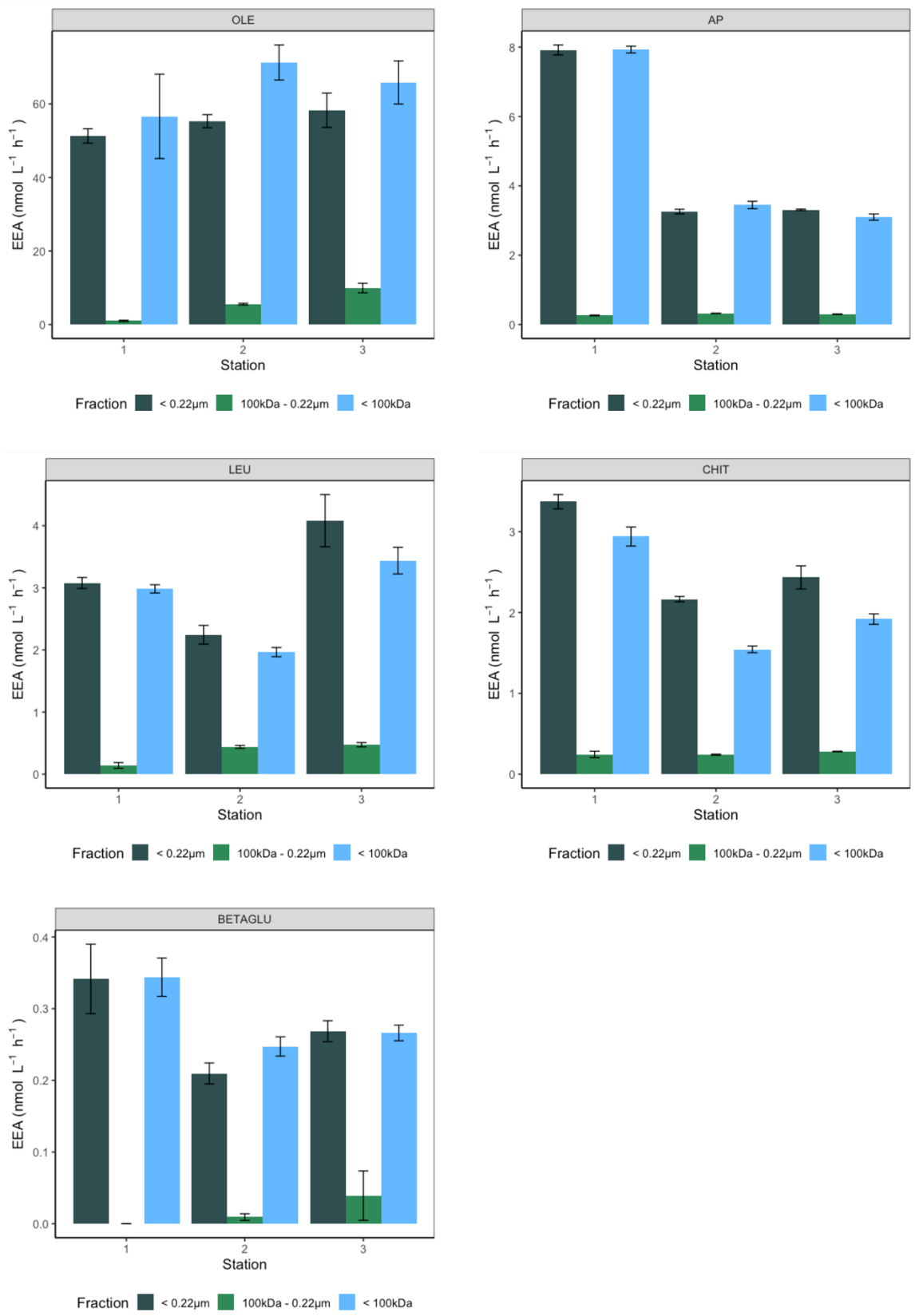

Figure 7. Extracellular enzymatic activity (EEA) measured in the cell-free fraction (< 0.22 µm), associated with nanoparticles (100 kDa - 0.22 µm), and in the nanoparticles-free fraction (< 100 kDa). The EEAs were measured on sampling stations 1-3 and results are shown from the third sampling event. OLE: olease, AP: alkaline phosphatase, LEU: leucine aminopeptidase, CHIT: chitinase, BETAGLU: β-glucosidase.

The highest contribution of EEA by nanoparticles to the total EEA of the cell-free fraction was seen for LEU (19.6%). For CHIT and OLE the contribution was on average 10 ± 2.4% and 10 ± 7.5% respectively. Nanoparticles contributed to the total EEA of the cell-free fraction with 7.5 ± 3.6% for AP. For BETAGLU the contribution of nanoparticles was on average 6.4 ± 7.5% (Table 2).

Table II. Percentage of nanoparticles (100 kDa - 0.22 µm) contributing to the total EEA of the cell-free (< 0.22 µm) fraction. LEU: leucine aminopeptidase, OLE: olease, CHIT: chitinase, AP: alkaline phosphatase, BETAGLU: β-glucosidase.

Enzyme	Percentage (%)
LEU	4.6 – 19.6
OLE	2.0 – 17.0
CHIT	7.3 – 11.6
AP	3.3 – 10.0
BETAGLU	0.0 – 14.6

Discussion

Over the course of the last ten years studies have shown that EVs are likely an important component in the complex microbial food web in marine environments. Laboratory studies indicate that EVs can be metabolized and that they harbor active ectoenzymes necessary for the degradation of complex substrates (Biller et al. 2014, Fadeev et al. 2023). However, little is known thus far on the abundance and fate of EVs in marine environments. Nekrouf et al. (2025) could identify some of the most common EV producers in the Mediterranean Sea like *Flavobacteria* and *Pelagibacter*. In this study, we determined the abundance and functional role of EVs in the natural environment of the North Adriatic Sea. This was done by measuring nutrient concentrations and EEA derived from nanoparticles and identifying what part of nanoparticles can be characterized as EV-like particles. As the concentrations of nanoparticles in the ocean are too low for most analysis, lengthy concentration, isolation and purification workflows are required. These processes - like any manipulation of samples - have their potential shortcomings which need to be taken into consideration when interpreting the results of this study.

Methodological considerations

Extracellular vesicles can be found in a variety of sizes commonly between 20 and 250 nm. They are extracted by filtration through a 0.22 µm membrane and concentrated via tangential flow filtration on a 100 kDa membrane. By default, there will always be smaller bacterial cells and high molecular weight aggregates that are able to pass the 0.22 µm barrier. Filtration also holds the risk of bursting cells on the membrane, releasing their contents into the filtrate. These residuals will then be included in the measurements of dissolved nutrients and EEA in the filtrate and the < 100 kDa outflow. By the design of our EEA approach, the EEA of the 100 kDa – 0.22 µm fraction and the < 100 kDa fraction together would need to add up to the EEA measured on the cell-fee (< 0.22 µm) samples. Yet for almost all samples EEA in the cell-free fraction and the nanoparticle-free fraction is almost the same. This might indicate potential damage of cells and hence artificial enrichment in hydrolases (Fig. 7).
Furthermore, EVs cannot be separated from virus-like particles by size fractionation. To study EVs, the nanoparticles need to be separated by density gradient fractionation. This method, however, is associated with high biomass losses as the particles need to be washed from iodixanol and resuspended in PBS. To accurately enumerate nanoparticles by NTA the concentrations should range between ~ 10^7 to 10^9 particles per mL (Nanosight NS300 User manual, MAN0541-01-EN-00, 2017). To reach these concentrations, the volume of seawater that would need to be filtered exceeded the available time frame of this analysis. Therefore, the enumeration had to be conducted on the lowest concentration of particles analyzable by NTA. This leads to decreased precision in particle counts and size estimates. The density gradient purification of nanoparticles further can lead to batch effect errors as likely occurred for the NTA results from station 3 on the second sampling event and station 1-3 on the third sampling event (Fig. 3). All four samples were purified in the same run. It is assumed that in the extraction of virus-like particles most particles could not be collected from the ultracentrifugation tubes leading to the low abundance of virus-like particles which should be typically in the range of 10^7 mL^{-1} for surface waters in the Northern Adriatic Sea (Weinbauer 2004). As these kinds of methodological biases could not be avoided, it is important to keep them in mind when analyzing these types of experimental data. However, it is reasonable to assume that the loss of virus-like and EV-like particles is similar during the concentration of nanoparticles. Hence the relation in abundance between these two categories of nanoparticles is likely not affected in the samples containing concentrated nanoparticles (100 kDa - 0.22 µm).

Ecological relevance of EVs

Ten - 30 % of nanoparticles in surface seawater can be characterized as EV-like particles. Nanoparticles defined as virus-like, were found in comparable concentration and size-range to particles defined as EV-like (Figs. 3 & 4). This is especially valid to take into account when enumerating viruses and phages by nucleic acid staining without former density gradient fractionation.

The detected concentrations of EV-like particles are comparable to concentrations in other oligotrophic surface waters (Biller et al. 2014, 2017, Nekrouf et al. 2025). These studies have also detected similar ratios of EV-like particles per bacterial cell in oligotrophic marine environments compared to the ratio measured during the course of this thesis (0.3 – 4.1 EV-like particles per bacterial cell). Unlike the findings of Nekrouf et al. (2025) in the Mediterranean Sea, we found only a weak correlation between the number of bacterial cells and EV-like particles (correlation coefficient 0.12). Surprisingly, the number of EV-like nanoparticles was negatively correlated with the bacterial carbon production (correlation coefficient -0.45). Overall, the average carbon production (3.0 ± 2.1 µg C L^{-1} d^{-1} (Fig. 2)) was lower than previous measurements of surface waters in the northern Adriatic where BCP was 9 µg C L^{-1} d^{-1} at 5 m depth. Our measurements are closer to the usual production at 20 m depth where rates of 5 µg C L^{-1} d^{-1} were measured at this time of the year (Orel et al. 2022, Tinta et al. 2015). Yet, it was surprising to see lower nanoparticle concentrations in samples with higher bacterial carbon production, generally indicating better bacterial growth conditions. However, having extracted samples from the depth of the thermocline, where the growth conditions might be disadvantageous compared to the surface waters, cells might produce more EVs as a stress response while BCP is decreasing. Thus far, many drivers of EV release have been investigated, yet no main regulator for vesicle production could be determined and it most likely differs for different microbes (Biller et al. 2023).

A spatial or temporal pattern of nanoparticle concentrations between sampling events and sampling stations could not be detected. Even though the sampling stations were chosen in different proximities to the coast we could also not see consistent patterns in dissolved nutrient concentrations or enzyme activities. However, increasing numbers of nanoparticles resulted in increasing concentrations of DOC, TDN, TSP (Figs. 2 & 5). To investigate the potential role of EVs as nutrient hotspots in the ocean DOC, TDN, and TSP concentrations derived from nanoparticles were evaluated. To achieve this, the measurements of the truly dissolved, nanoparticle-depleted (< 100 kDa) samples were subtracted from the measurements of the EV-containing size fraction (100 kDa - 0.22 µm). By subtracting the truly dissolved "background", it was discovered that roughly 6% of DOC, TDN and TSP are contained in nanoparticles (Fig. 5, Table 1). This shows that a small, but substantial fraction of dissolved nutrients is actually associated with high molecular weight nanoparticles, which includes microbial extracellular vesicles. Further, our findings indicate that nanoparticles not only harbor nutrients, but are also enriched in nitrogen compared to the surrounding environment (Table 1). Encapsulated in a protective membrane it can be assumed these nutrient aggregates are somewhat protected against degradation and diffusion (Biller et al. 2014, Deatherage & Cookson 2012).

Another important aspect of the ecological role of extracellular vesicles is their potential to hydrolyze complex organic compounds. This was investigated by comparing the EEA of major hydrolases in cell-free (< 0.22 µm) seawater to the EEA directly associated with nanoparticles (100 kDa - 0.22 µm). Former studies have shown that 20 – 50 % of the total EEA is contributed by the nanoparticle containing size fraction (Baltar et al. 2019, Fadeev et al. 2023). From the five hydrolases investigated,

only β-glucosidase appeared to be truly dissolved and not attached to nanoparticles. Even though the EEA for BETAGLU is relatively high on station 3, the big standard deviation indicates that it is not a reliable value. The highest EEA measured from nanoparticles alone was measured for olease, indicating that the detected nanoparticles might be a part of the lipid cycling in oligotrophic marine environments (Fig. 7). The highest contribution of nanoparticles to the total EEA of the cell-free fraction was seen for LEU with almost 20% (Table 2). On average for LEU, OLE, and CHIT nanoparticles contributed approx. 10% to the total measured EEA in the cell-free size fraction (< 0.22 µm) (Table 2). This results indicate that at least a part of the active extracellular enzymes is not truly dissolved, but associated with nanoparticles. Measuring extracellular activity that is associated with nanoparticles supports the hypothesis that nanoparticles such as EV-like nanoparticles can support the hydrolyzation of different complex organic compounds.

Conclusion and future perspectives

It has been evident that extracellular vesicles can have various functions in the marine environment. In this contribution we could show that EVs make up a substantial amount of the total nanoparticles found in the Northern Adriatic Sea. Encapsulating a small, yet considerable amount of nutrients and harboring concentrated active enzymes, nanoparticles can both work as nutrient storage as well as for targeting complex substrates for degradation in oligotrophic marine environments.

To further investigate this, it would be very interesting to see how much of the nutrients can be extracted from the purified EVs directly. Assuming 6% of the measured nutrients are derived from nanoparticles it would result in 2% of nutrients solely from EV-like particles. However, being composed of different component concentrations, this is only a crude estimate. In order to examine such composition reliably, the concentration of EV-like particles would have to be a lot higher, which is yet challenging with the current methods for EV extraction from natural seawater samples. The same holds true for EEA assays on purified EV-like particles from the natural environment. As a comparison to this study a valuable extension could be to focus on one sample only, but increase the sample volume at least 10-fold and repeat nutrient and EEA analyses on purified EV-like particles.

List of figures and tables

References

Adamo, G., Fierli, D., Romancino, D. P., Picciotto, S., Barone, M. E., Aranyos, A., Bozic, D., Morsbach, S., Raccosta, S., Stanly, C., Paganini, C., Gai, M., Cusimano, A., Martorana, V., Noto, R., Carrotta, R., Librizzi, F., Randazzo, L., & Bongiovanni, A. (2021). Nanoalgosomes: Introducing extracellular vesicles produced by microalgae. Journal of extracellular vesicles, 10(6), e12081.

Awwa, A. P. H. A. (1998). Standard methods for the examination of water and wastewater. *Washington, DC Standard Methods for the Examination of Water and Wastewater*, *20*.

Bachurski, D., Schuldner, M., Nguyen, P. H., Malz, A., Reiners, K. S., Grenzi, P. C., Babaz, F., Schauss, A. C., Hansen, H. P., Hallek, M., & Pogge von Strandmann, E. (2019). Extracellular vesicle measurements with nanoparticle tracking analysis–An accuracy and repeatability comparison between NanoSight NS300 and ZetaView. Journal of extracellular vesicles, 8(1), 1596016.

Baeza, N., & Mercade, E. (2020). Relationship between membrane vesicles, extracellular ATP and biofilm formation in Antarctic Gram-negative bacteria. Microbial ecology, 81(3), 645-656.

Baltar, F., De Corte, D., Thomson, B., & Yokokawa, T. (2019). Teasing apart the different size pools of extracellular enzymatic activity in the ocean. *Science of The Total Environment*, *660*, 690-696.

Bauman, S. J., & Kuehn, M. J. (2006). Purification of outer membrane vesicles from *Pseudomonas aeruginosa* and their activation of an IL-8 response. Microbes and infection, 8(9-10), 2400-2408.

Biller, S. J., Schubotz, F., Roggensack, S. E., Thompson, A. W., Summons, R. E., & Chisholm, S. W. (2014). Bacterial vesicles in marine ecosystems. Science, 343(6167), 183-186.

Biller, S. J., McDaniel, L. D., Breitbart, M., Rogers, E., Paul, J. H., & Chisholm, S. W. (2017). Membrane vesicles in sea water: heterogeneous DNA content and implications for viral abundance estimates. *The ISME Journal*, *11*(2), 394-404.

Biller, S. J. (2020). Extracellular Vesicles in the Environment. Bacterial Membrane Vesicles, 75-99.

Biller, S. J., Coe, A., Arellano, A. A., Dooley, K., Gong, J. S., Yeager, E. A., Becker, J. W., & Chisholm, S. W. (2022). Environmental and taxonomic drivers of bacterial extracellular vesicle production in marine ecosystems. bioRxiv.

Biller, S. J., Lundeen, R. A., Hmelo, L. R., Becker, K. W., Arellano, A. A., Dooley, K., Heal, K. R., Carlson, L. T., Van Mooy, B. A. S., Ingalls, A. E., & Chisholm, S. W. (2022). *Prochlorococcus* extracellular vesicles: molecular composition and adsorption to diverse microbes. Environmental Microbiology, 24(1), 420-435.

Biller, S. J., McDaniel, L. D., Breitbart, M., Rogers, E., Paul, J. H., & Chisholm, S. W. (2017). Membrane vesicles in sea water: heterogeneous DNA content and implications for viral abundance estimates. The ISME Journal, 11(2), 394-404.

Bos, M. P., Robert, V., & Tommassen, J. (2007). Biogenesis of the gram-negative bacterial outer membrane. Annu. Rev. Microbiol., 61, 191-214.

Brussaard, C. P. (2004). Optimization of procedures for counting viruses by flow cytometry. *Applied and Environmental Microbiology*, *70*(3), 1506-1513.

Celussi, M., & Del Negro, P. (2012). Microbial degradation at a shallow coastal site: Long-term spectra and rates of exoenzymatic activities in the NE Adriatic Sea. Estuarine, Coastal and Shelf Science, 115, 75–86.

Celussi, M., Fabbro, C., Bastianini, M., Urbani, R., & Del Negro, P. (2015). Polysaccharide degradation and utilisation during a spring phytoplankton bloom in the northwestern Adriatic Sea. Hydrobiologia, 757, 209-222.

Choi, D. H., Kwon, Y. M., Chiura, H. X., Yang, E. C., Bae, S. S., Kang, S. G., Lee, J. H., Yoon, H. S., & Kim, S. J. (2015). Extracellular vesicles of the hyperthermophilic archaeon "*Thermococcus onnurineus*" NA1T. Applied and environmental microbiology, 81(14), 4591-4599.

Deatherage, B. L., & Cookson, B., T. (2012). Membrane vesicle release in bacteria, eukaryotes, and archaea: a conserved yet underappreciated aspect of microbial life. Infection and immunity, 80(6), 1948-1957.

De Rond, L., Van Der Pol, E., Hau, C. M., Varga, Z., Sturk, A., Van Leeuwen, T. G., Nieuwland, R., & Coumans, F. A. (2018). Comparison of generic fluorescent markers for detection of extracellular vesicles by flow cytometry. Clinical Chemistry, 64(4), 680-689.

Ellis, T. N., & Kuehn, M. J. (2010). Virulence and immunomodulatory roles of bacterial outer membrane vesicles. Microbiology and molecular biology reviews, 74(1), 81-94.

Evtushenko, E. G., Bagrov, D. V., Lazarev, V. N., Livshits, M. A., & Khomyakova, E. (2020). Adsorption of extracellular vesicles onto the tube walls during storage in solution. PloS one, 15(12), e0243738.

Fadeev, E., Carpaneto Bastos, C., Hennenfeind, J. H., Biller, S. J., Sher, D., Wietz, M., & Herndl, G. J. (2023). Characterization of membrane vesicles in *Alteromonas macleodii* indicates potential roles in their copiotrophic lifestyle. Microlife, 4, uqac025.

Frias, A., Manresa, A., de Oliveira, E., López-Iglesias, C., & Mercade, E. (2010). Membrane vesicles: a common feature in the extracellular matter of cold-adapted Antarctic bacteria. Microbial Ecology, 59(3), 476-486.

Gardiner, C., Ferreira, Y. J., Dragovic, R. A., Redman, C. W., & Sargent, I. L. (2013). Extracellular vesicle sizing and enumeration by nanoparticle tracking analysis. Journal of extracellular vesicles, 2(1), 19671.

Hansell, D. A., & Carlson, C. A. (1998). Net community production of dissolved organic carbon. *Global Biogeochemical Cycles*, *12*(3), 443-453.

Hoppe, H., G. (1993). Use of fluorogenic model substrates for extracellular enzyme activity (EEA) measurement of bacteria. Kemp PF, Sherr BF, Sherr EB, Cole JJ (eds) Current methods in aquatic microbial ecology. CRC Press, Boca Raton, 423–431.

Hagemann, S., Stöger, L., Kappelmann, M., Hassl, I., Ellinger, A., & Velimirov, B. (2013). DNA-bearing membrane vesicles produced by *Ahrensia kielensis* and *Pseudoalteromonas marina*. Journal of basic microbiology, 54(10), 1062-1072.

Horstman, A. L., & Kuehn, M. J. (2000). Enterotoxigenic *Escherichia coli* secretes active heat-labile enterotoxin via outer membrane vesicles. Journal of Biological Chemistry, 275(17), 12489-12496.

Kulp, A., & Kuehn, M. J. (2010). Biological functions and biogenesis of secreted bacterial outer membrane vesicles. Annual review of microbiology, 64, 163.

Kwon, Y. M., Patra, A. K., Chiura, H. X., & Kim, S. J. (2019). Production of extracellular vesicles with light-induced proton pump activity by proteorhodopsin-containing marine bacteria. MicrobiologyOpen, 8(8), e00808.

Lee, S., & Fuhrman, J. A. (1987). Relationships between biovolume and biomass of naturally derived marine bacterioplankton. Applied and environmental microbiology, 53(6), 1298-1303.

Li, J., Azam, F., & Zhang, S. (2016). Outer membrane vesicles containing signalling molecules and active hydrolytic enzymes released by a coral pathogen *Vibrio shilonii AK1*. Environmental microbiology, 18(11), 3850-3866.

López-Pérez, M., Gonzaga, A., Martin-Cuadrado, A. B., Onyshchenko, O., Ghavidel, A., Ghai, R., & Rodriguez-Valera, F. (2012). Genomes of surface isolates of *Alteromonas macleodii*: the life of a widespread marine opportunistic copiotroph. Scientific Reports, 2(1), 1-11.

Lynch, J. B., & Alegado, R. A. (2017). Spheres of hope, packets of doom: the good and bad of outer membrane vesicles in interspecies and ecological dynamics. Journal of bacteriology, 199(15), e00012-17.

Malačič, V., Celio, M., Čermelj, B., Bussani, A., & Comici, C. (2006). Interannual evolution of seasonal thermohaline properties in the Gulf of Trieste (northern Adriatic) 1991–2003. Journal of Geophysical Research: Oceans, 111(C8).

Manning, A. J., & Kuehn, M. J. (2011). Contribution of bacterial outer membrane vesicles to innate bacterial defense. BMC microbiology, 11(1), 1-15.

Marie, D., Partensky, F., Vaulot, D., & Brussaard, C. (1999). Enumeration of phytoplankton, bacteria, and viruses in marine samples. *Current protocols in cytometry*, *10*(1), 11-11.

McBroom, A. J., Johnson, A. P., Vemulapalli, S., & Kuehn, M. J. (2006). Outer membrane vesicle production by *Escherichia coli* is independent of membrane instability. Journal of bacteriology, 188(15), 5385-5392.

McBroom, A. J., & Kuehn, M. J. (2005). Outer membrane vesicles. EcoSal Plus, 1(2).

McBroom, A. J., & Kuehn, M. J. (2007). Release of outer membrane vesicles by Gram-negative bacteria is a novel envelope stress response. Molecular microbiology, 63(2), 545-558.

MISEV (2022). Minimal information for studies of extracellular vesicles 2022 (MISEV2022): a position statement of the International Society for Extracellular Vesicles and update of the MISEV2018 guidelines. Draft Manuscript.

Naval, P., & Chandra, T. S. (2019). Characterization of membrane vesicles secreted by seaweed associated bacterium *Alteromonas macleodii KS62*. Biochemical and biophysical research communications, 514(2), 422-427.

Nagakubo, T., Nomura, N., & Toyofuku, M. (2020). Cracking open bacterial membrane vesicles. Frontiers in Microbiology, 10, 3026.

Nekrouf, N. A., Maestre-Carballa, L., Lluesma-Gomez, M., Martinez-Hernandez, F., & Martinez-Garcia, M. (2025). Annual dynamics and metagenomics of marine vesicles: One more layer of complexity in the dissolved organic fraction. *Limnology and Oceanography*.

Orel, N., Fadeev, E., Klun, K., Ličer, M., Tinta, T., & Turk, V. (2022). Bacterial indicators are ubiquitous members of pelagic microbiome in anthropogenically impacted coastal ecosystem. *Frontiers in microbiology*, *12*, 765091.

Schatz, D., Rosenwasser, S., Malitsky, S., Wolf, S. G., Feldmesser, E., & Vardi, A. (2017). Communication via extracellular vesicles enhances viral infection of a cosmopolitan alga. Nature Microbiology, 2(11), 1485-1492.

Schatz, D., & Vardi, A. (2018). Extracellular vesicles—new players in cell–cell communication in aquatic environments. Current opinion in microbiology, 43, 148-154.

Schooling, S. R., & Beveridge, T. J. (2006). Membrane vesicles: an overlooked component of the matrices of biofilms. Journal of bacteriology, 188(16), 5945-5957.

Schwechheimer, C., & Kuehn, M. J. (2015). Outer-membrane vesicles from Gram-negative bacteria: biogenesis and functions. Nature reviews microbiology, 13(10), 605-619.

Simon, M., & Azam, F. (1989). Protein content and protein synthesis rates of planktonic marine bacteria. Marine ecology progress series, 201-213.

Smith, D. C., & Azam, F. (1992). A simple, economical method for measuring bacterial protein synthesis rates in seawater using 3H-leucine. Marine microbial food webs, 6(2), 107-114.

Soler, N., Marguet, E., Verbavatz, J. M., & Forterre, P. (2008). Virus-like vesicles and extracellular DNA produced by hyperthermophilic archaea of the order *Thermococcales*. Research in Microbiology, 159(5), 390-399.

Soler, N., Krupovic, M., Marguet, E., & Forterre, P. (2015). Membrane vesicles in natural environments: a major challenge in viral ecology. The ISME Journal, 9(4), 793-796.

Théry, C., Witwer, K. W., Aikawa, E., et al. (2018). Minimal information for studies of extracellular vesicles 2018 (MISEV2018): a position statement of the International Society for Extracellular Vesicles and update of the MISEV2014 guidelines. Journal of extracellular vesicles, 7(1), 1535750.

Tinta, T., Vojvoda, J., Mozetič, P., Talaber, I., Vodopivec, M., Malfatti, F., & Turk, V. (2015). Bacterial community shift is induced by dynamic environmental parameters in a changing coastal ecosystem (northern Adriatic, northeastern Mediterranean Sea) – a 2-year time-series study. *Environmental microbiology*, *17*(10), 3581-3596.

Toyofuku, M. (2019). Bacterial communication through membrane vesicles. *Bioscience, Biotechnology, and Biochemistry*, *83*(9), 1599-1605.

Van Deun, J., Mestdagh, P., Sormunen, R., Cocquyt, V., Vermaelen, K., Vandesompele, J., Bracke, M., De Wever, O., & Hendrix, A. (2014). The impact of disparate isolation methods for extracellular vesicles on downstream RNA profiling. Journal of extracellular vesicles, 3(1), 24858.

Verdugo, P., Alldredge, A. L., Azam, F., Kirchman, D. L., Passow, U., & Santschi, P. H. (2004). The oceanic gel phase: a bridge in the DOM-POM continuum. Marine Chemistry, 92(1-4), 67-85.

Weinbauer, M. G. (2004). Ecology of prokaryotic viruses. *FEMS microbiology reviews*, *28*(2), 127-181.